

THREE-DIMENSIONAL MAGNETOHYDRODYNAMIC SIMULATIONS OF RELATIVISTIC JETS INJECTED ALONG A MAGNETIC FIELD

KEN-ICHI NISHIKAWA,¹ SHINJI KOIDE,² JUN-ICHI SAKAI,² DIMITRIS M. CHRISTODOULOU,¹ HÉLÈNE SOL,³ AND ROBERT L. MUTEL⁴

Received 1997 November 27; accepted 1997 April 18

ABSTRACT

We present the first numerical simulations of moderately hot, supersonic jets propagating initially along the field lines of a denser magnetized background medium with Lorentz factor $W = 4.56$ and evolving in a four-dimensional spacetime. Compared with previous simulations in two spatial dimensions, the resulting structure and kinematics differ noticeably: the density of the Mach disk is lower, and the head speed is smaller. This is because the impacted ambient fluid and its embedded magnetic field make efficient use of the third spatial dimension as they are deflected circularly off of the head of the jet. As a result, a significant magnetic field component normal to the jet is created near the head. If the field is strong, backflow and field reversals are strongly suppressed; upstream, the field closes back on the surface of the beam and assists the collimation of the jet. If the field is weak, backflow and field reversals are more pronounced, although still not as extended as in the corresponding plane-parallel case. In all studied cases, the high-pressure region is localized near the jet head irrespective of the presence/strength of the magnetic field, and the head decelerates efficiently by transferring momentum to the background fluid that recedes along a thin bow shock in all directions. Furthermore, two oppositely directed currents circle near the surface of the cylindrical beam, and a third current circles on the bow shock. These preliminary results underline the importance of performing fully three-dimensional simulations to investigate the morphology and propagation of relativistic extragalactic jets.

Subject headings: galaxies: jets — magnetic fields — methods: numerical — MHD — relativity

1. INTRODUCTION

There is now ample evidence that extragalactic jets at scales of 10–100 pc flow out of active galactic nuclei at speeds comparable to the speed of light ($v \approx c$) and that the outflows maintain significant relativistic speeds ($v \sim 0.6c$ – $0.8c$) out to scales of at least 1 kpc. The evidence comes from modeling VLBI observations of superluminal motions in many (>40) quasars and BL Lacertae objects (Gabuzda, Wardle, & Roberts 1989; Mutel et al. 1990; Cawthorne 1991; Davis, Unwin, & Muxlow 1991; Gabuzda et al. 1992; Hummel et al. 1992a, 1992b; Ghisellini et al. 1993; Biretta 1993; Biretta, Zhou, & Owen 1995; Wardle & Aaron 1996) and from the detection of intraday variability in more than 25% of the known compact radio sources (see Qian et al. 1991, 1996 and Krichbaum, Quirrenbach, & Witzel 1992 in conjunction with the theoretical estimates of Begelman, Rees, & Sikora 1994). These observations indicate that the bulk of the outflowing material must be moving at Lorentz factors of $W \sim 10$ ($v = 0.995c$) or faster ($W \sim 30$ – 100 and $v > 0.999c$, according to Begelman et al. 1994). Polarization measurements and modeling also reveal that the jets are magnetized and that the magnetic fields should be dynamically important in some particular FR II radio sources and in BL Lacertae objects (Clarke 1993; Laing 1996; Koide et al. 1996c and references therein).

Including the above effects in simulations of cylindrical fluid

jets constitutes an exercise in two-dimensional relativistic magnetohydrodynamics (RMHD)—and this is neglecting three-dimensional effects as well as radiation processes that give rise to the observed synchrotron emission (but see Gómez et al. 1995, Komissarov & Falle 1996a, and Georganopoulos & Marscher 1996 for radiative models). The inclusion of relativistic effects, in particular, is a recent endeavor in jet hydrodynamics. Following the older, brave effort of Yokosawa, Ikeuchi, & Sakashita (1982), two-dimensional, special relativistic simulations have been carried out over the past 4 years (van Putten 1993; Duncan & Hughes 1994; Martí, Müller, & Ibáñez 1994; Martí et al. 1995, 1996; Koide, Nishikawa, & Mutel 1996a; Komissarov & Falle 1996b). Furthermore, the study of frozen-in magnetic fields and of the third spatial dimension in the relativistic domain is just beginning (Koide et al. 1996a, van Putten 1996, and this Letter, respectively).

These effects have already been included in nonrelativistic jet simulations and have led to successful comparisons between numerically predicted and actually observed characteristics (see, e.g., Balsara & Norman 1992, Hardee & Clarke 1992, 1995, and Hardee, Clarke, & Howell 1995 for three-dimensional hydrodynamic simulations and Clarke, Norman, & Burns 1986, Stone & Norman 1992, Clarke 1993, Hardee & Clarke 1995, Hardee 1996, and Koide et al. 1996c for two- and three-dimensional magnetohydrodynamic [MHD] simulations). Reviews covering these topics have been written by Burns, Norman, & Clarke (1991) and by Norman (1993, 1996). Despite complications and changes in the details of jet propagation, no major surprises emerged from the consideration of active or passive magnetic fields. The most interesting results obtained from three-dimensional MHD simulations are the higher degree of beam collimation effected by dynamically evolving, strong toroidal magnetic fields as well as the creation of compact “nose cones” in magnetically confined jets and

¹ Department of Physics and Astronomy, Louisiana State University, Baton Rouge, LA 70803; kenichi@rouge.phys.lsu.edu, dchristo@rouge.phys.lsu.edu.

² Laboratory of Plasma Physics and Fusion Science, Faculty of Engineering, Toyama University, Gofuku, Toyama 930, Japan; koidesin@ecs.toyama-u.ac.jp, sakaijun@ecs.toyama-u.ac.jp.

³ DARC, Observatoire de Paris-Section de Meudon, Place Jules Janssen, F-92195 Meudon Cedex, France; Helene.Sol@obspm.fr.

⁴ Department of Physics and Astronomy, University of Iowa, 203 Van Allen Hall, Iowa City, IA 52242; rlm@astro.physics.uiowa.edu.

their shedding to the side before they grow too large (Clarke 1993). On the other hand, purely hydrodynamic three-dimensional simulations revealed some rather surprising structural changes: jets in three dimensions are not intrinsically as stable as in a two-dimensional geometry because their beams are deflected, splatter, and create two hot spots instead of a Mach disk; their bow shocks are distorted accordingly; and the backflow in their asymmetric cocoons is more turbulent, with vortical eddies maintaining fully three-dimensional structures (e.g., Norman 1993).

In this Letter, we discuss new results obtained from fully three-dimensional RMHD jet simulations carried out for a brief period of time and at a modest grid resolution of 101^3 zones. In § 2, we demonstrate the effects of the included, third spatial dimension through comparisons with two-dimensional results that we obtained in a plane-parallel geometry (Koide et al. 1996a). A summary of our conclusions is presented in § 3.

2. INITIAL CONDITIONS AND NUMERICAL RESULTS

The relevant RMHD equations and the employed, three-dimensional computer program have been briefly introduced by Koide et al. (1996a, hereafter KNM). A detailed description of the numerical techniques and related test problems in the relativistic domain are given in Koide, Nishikawa, & Mutel (1996b). For the present simulations, we employ a Cartesian XYZ grid with 101 equally spaced zones in each direction. The computational box is a cube that occupies the region $0 \leq X \leq 20$, $-10 \leq Y, Z \leq 10$. This box is filled uniformly with fluid of rest mass density $\rho_a = 1$, pressure $P_a = 0.6$, and specific energy $\epsilon_a = 0.9$; a uniform magnetic field B is also embedded and points initially in the X -direction. At times, $t \geq 0$, jet material of rest mass density $\rho_j = 0.3$ ($\eta \equiv \rho_j/\rho_a = 0.3$), and specific energy $\epsilon_j = 3$ is injected in the X -direction from an orifice at $X = 0$, $Y^2 + Z^2 \leq 1$. The jet's proper pressure is initially equal to the thermal pressure of the ambient medium. No symmetry is assumed across any of the boundaries during evolution. In addition, fixed-inflow and radiative boundary conditions are implemented at the $X = 0$ surface and at all the other surfaces, respectively. Thus, the propagation of the jet can be followed only for a relatively brief period of time spanning ≤ 20 initial jet radii. With this setup and resolution, we do not hope to follow the long-term evolution of the jets that might lead to pronounced asymmetries and head fluctuations, and we concentrate on the structure and kinematics that develop near and around the surfaces of the beams.

Computations are currently performed on the Power Challenge of the National Center for Supercomputing Applications with over 1 Gbyte dynamic memory and require 2.5 minutes of CPU time per time step. The present simulations were designed for a direct comparison with the corresponding two-dimensional simulations presented by KNM. For this reason, we express velocities in units of the sound speed v_s in the ambient medium, and we measure time in units of τ_s , the transit time of a sound wave over unit distance. In addition, we choose an adiabatic index of $\gamma = 5/3$ for the fluid and an injection speed v_j that leads to a proper Mach number of $M_j \equiv v_j/v_s = 4$ and a Lorentz factor of $W_j = (1 - v_j^2/c^2)^{-1/2} = 4.56$ ($v_j/c = 0.9756$ for $c = 4.1v_s$).

So far, we have performed three runs characterized by various strengths of the initial magnetic field: in run A, the energy density of the field, $B^2/2$, was equal to $5/9$ of the internal energy density, $\rho_a \epsilon_a$, of the ambient medium (Alfvén

speed $v_A \equiv B\rho^{-1/2} = v_s$); in run B, the energy density of the field was reduced by a factor of 16 ($v_A = 0.25v_s$); and in run C, there was no magnetic field. Because the results from runs B and C are similar, we describe here only the first two runs with a strong and a weak initial magnetic field, respectively.

Figures 1a and 1b and Figures 1c and 1d (Plate L4) show various MHD variables on the $Y = 0$ plane at $t = 8.5\tau_s$ for runs A and B, respectively. Figures 1a and 1c depict the rest mass density and the velocity, while Figures 1b and 1d depict the thermal pressure and the magnetic field. (Horizontal $[XY]$ cross sections at $Z = 0$ reveal very much the same morphology, while YZ cross sections show the overall axisymmetry of the jets.) In both cases, the Mach disks (Figs. 1a and 1c) are almost at the same location, $X \approx 17$, because the average propagation speeds of the relativistic jet heads are almost the same: $v_h = 2.06v_s$. (In more detail, the heads slow down to the following average speeds: $v_h = 2.17v_s$ for $0 < t < 3.0\tau_s$, $2.10v_s$ for $3.0\tau_s < t < 6.0\tau_s$, and $1.88v_s$ for $6.0\tau_s < t < 8.5\tau_s$.) Although higher than the one-dimensional, nonrelativistic estimate of $v_h = \eta^{1/2}(1 + \eta^{1/2})^{-1}v_j = 1.42v_s$, this average speed is significantly smaller than both the two-dimensional value of $v_h = 2.67v_s$ found by KNM and the corresponding one-dimensional, relativistic, nonmagnetic estimate (e.g., Martí et al. 1996) of $v_h = \eta^{1/2}(1 + \eta^{1/2})^{-1}v_j = 2.92v_s$, where the relativistic inertia ratio $\eta_R \equiv \eta(h_j/h_a)W_j^2 = 7.42$ and $h \equiv 1 + (\epsilon + P/\rho)/c^2$ denotes the relativistic specific enthalpy. The observed head speed is in between the above relativistic and nonrelativistic estimates. This outcome is clearly due to a combination of relativistic and three-dimensional effects: Lorentz contraction increases the effective mass density of the jet, and hence its thrust and average speed, but the head of the beam is decelerated by the ambient medium more strongly in three dimensions than in two dimensions; hence, an average propagation efficiency of only $2.06/2.92 = 70\%$ is achieved because of more efficient momentum transfer to the impacted, three-dimensional fluid.

Comparing the two cases, the transverse propagation of the bow shock is faster in run A (Figs. 1a and 1b) because the fast magnetosonic waves are faster in the strongly magnetized medium. Also, the width of the bow shock in run A is smaller because the shocked ambient flow is not affected substantially by backflow as the magnetic field is deflected by the head less than in run B (see Fig. 2 below). In relation to the two-dimensional case, however, the widths of both three-dimensional bow shocks are smaller, and their tips are closer to the beams (see Figs. 1 and 2 in KNM).

The density of the Mach disk and the head pressure are both higher by $\sim 10\%$ in the weak-field run B. In both runs, however, the high-pressure region is strongly localized around the head (Figs. 1b and 1d). This feature is also due to three-dimensional effects because it is not observed in the two-dimensional simulations of KNM. The localization occurs because there is no preferred direction for momentum transfer in the three-dimensional runs, leading to more efficient matter transport away from the head.

Figure 1c shows “wings” of pronounced backflow forming beside the jet in run B. With the exception of a thin surface layer behind the head, no such feature develops in the strong-field case. The absence of backflow in Figure 1a is similar to the result obtained by Martí et al. (1996) from a nonmagnetic, two-dimensional simulation of a considerably hotter jet. It seems then that either a strong, aligned magnetic field in the ambient medium or a high, internal, specific energy

in the jet can independently prevent backflow and cocoon turbulence.

One of the best ways to illustrate structural details on the head and the surface of the jet is to trace the magnetic field lines in three-dimensional space. This is shown in Figure 2 (Plate L00) for runs A and B at $t = 8.5\tau_s$. The observer is located in front and to the side of the approaching beam. The following features are readily apparent: (1) bending of the field lines (rotational discontinuity) at the location of the bow shock; (2) a flared region behind the head, inside of which the ambient field has been canceled by a current induced around the beam; and (3) confining, straight field lines upstream along the surface of the beam in run A and pronounced field-line reversals in run B (*red curves*).

In run A, the strong magnetic field that is pushed away by the propagating beam is deflected almost circularly; as a result, it develops significant normal components (on the Y - Z plane), comparable to the X -components. The field closes back on the beam upstream and contributes to the confinement of the exceptionally thin and internally featureless jet (Figs. 1a and 2a). Although deflected in a similar fashion, the field in run B is too weak to play the same role. Thus, the weak magnetic field in run B does not influence the propagation and collimation of the jet that evolves very much as in the nonmagnetic run C and results in the formation of a significantly less confined beam (Figs. 1c and 2b). In addition, Figure 2b shows that the reversal of field lines in run B is limited near the surface of the beam. By comparison, Figure 2a shows only a hint of very small field reversals in run A. In the corresponding two-dimensional cases (KNM), both field-line reversals and backflowing wings are more pronounced and more extended.

The regions where the magnetic field is near zero (Figs. 1b and 1d) indicate the location of the induced current whose density distribution $\mathbf{J} \equiv \nabla \times \mathbf{B}$ is quite complex, as shown in Figure 3 (Plate L5): two distinct, concentric, roughly cylindrical surfaces with toroidal current form near the surface of the beam and approach each other near the head, and another current circulates on the bow shock. The currents on the bow shock and the inner cylindrical surface have the same polarity, which is opposite to that of the current on the outer cylindrical surface. All three currents are generated from the interaction of the jet with the ambient plasma in places where the magnetic field lines are bent or canceled, as described above.

We finally note that a deviation of the beam from its original path has been observed during these simulations, and longer time integrations are needed in order to find out whether this effect is the beginning of nonlinear head oscillations analogous to those seen in nonmagnetic, nonrelativistic, three-dimensional jets (Norman 1993). At the endpoint of our runs, the

heads of the jets are displaced by a few grid cells relative to the original direction of propagation. A displacement of this magnitude is not sufficient to produce pronounced asymmetries in the leading section of the beam. Its presence, however, is revealed on the bow shock in Figure 3, where the circulating current appears to be off-centered.

3. CONCLUSIONS

Fully three-dimensional RMHD jet simulations of modest grid resolution (101^3 zones) and duration (up to $t = 8.5\tau_s$) confirm the general results obtained from previous two-dimensional simulations performed with an initially aligned magnetic field or in the absence of a field: both the relativistic terms in the RMHD equations and the presence of strong magnetic fields efficiently assist the collimation of propagating jets that appear to be thinner when both effects are included. The new simulations indicate that, in addition, consideration of all three spatial dimensions is necessary in order to capture correctly the morphology and kinematics of the jets.

In contrast to the two-dimensional case, we have found that moderately hot, three-dimensional relativistic beams decelerate more efficiently, develop no internal structures, and maintain circular currents at parts of their surfaces and small localized heads of lower density and pressure, and that the associated bow shocks are considerably thinner and stay closer to the beams. Furthermore, the jets are better collimated and show no strong backflows or significant field reversals in the presence of dynamically important ambient magnetic fields. A strong magnetic field is temporarily pushed away by the head almost axisymmetrically but returns to confine the beam farther upstream. In the cases of weak or no magnetic field, backflowing wings and pronounced field reversals do develop, but they are not as strong as in the corresponding two-dimensional plane-parallel cases studied by KNM; hence, the lesser but significant confinement of the jet is entirely due to relativistic effects.

We note that the magnetic field in this study is initially aligned with the jet and that this configuration does not resist the propagation of the beam. The study of three-dimensional RMHD jets injected into an oblique ambient magnetic field is currently in progress.

We thank an anonymous referee for constructive comments and suggestions. This work was supported in part by the US-Japan cooperative science program JSPS and by NSF (INT 92-17650); by NSF grants ATM 91-19814, ATM 91-21116, and AST 95-28424; by NASA grant NAG5-2777; and by supercomputing grants at NCSA, PSC, and SDSC.

REFERENCES

- Balsara, D. S., & Norman, M. L. 1992, *ApJ*, 393, 631
 Begelman, M. C., Rees, M. J., & Sikora, M. 1994, *ApJ*, 429, L57
 Biretta, J. 1993, in *Astrophysical Jets*, ed. D. Burgarella, M. Livio, & C. O'Dea (Cambridge: Cambridge Univ. Press), 263
 Biretta, J. A., Zhou, F., & Owen, F. N. 1995, *ApJ*, 447, 582
 Burns, J. O., Norman, M. L., & Clarke, D. A. 1991, *Science*, 253, 522
 Cawthorne, T. V. 1991, in *Beams and Jets in Astrophysics*, ed. P. A. Hughes (Cambridge: Cambridge Univ. Press), 187
 Clarke, D. A. 1993, in *Jets in Extragalactic Radio Sources*, ed. H.-J. Röser & K. Meisenheimer (Berlin: Springer), 243
 Clarke, D. A., Norman, M. L., & Burns, J. O. 1986, *ApJ*, 311, L63
 Davis, R. J., Unwin, S. C., & Muxlow, T. W. B. 1991, *Nature*, 354, 374
 Duncan, G. C., & Hughes, P. A. 1994, *ApJ*, 436, L119
 Gabuzda, D. C., Cawthorne, T. V., Roberts, D. H., & Wardle, J. F. C. 1992, *ApJ*, 388, 40
 Gabuzda, D. C., Wardle, J. F. C., & Roberts, D. H. 1989, *ApJ*, 336, L59
 Georganopoulos, M., & Marscher, A. P. 1996, in *ASP Conf. Ser. 100, Energy Transport in Radio Galaxies and Quasars*, ed. P. E. Hardee, A. H. Bridle, & J. A. Zensus (San Francisco: ASP), 67
 Ghisellini, G., Padovani, P., Celotti, A., & Maraschi, L. 1993, *ApJ*, 407, 65
 Gómez, J. L., Martí, J. M., Marscher, A. P., Ibáñez, J. M., & Marcaide, J. M. 1995, *ApJ*, 449, L19
 Hardee, P. E. 1996, in *ASP Conf. Ser. 100, Energy Transport in Radio Galaxies and Quasars*, ed. P. E. Hardee, A. H. Bridle, & J. A. Zensus (San Francisco: ASP), 273
 Hardee, P. E., & Clarke, D. A. 1992, *ApJ*, 400, L9
 ———. 1995, *ApJ*, 451, L25
 Hardee, P. E., Clarke, D. A., & Howell, D. A. 1995, *ApJ*, 441, 644
 Hummel, C. A., Muxlow, T. W. B., Krichbaum, T. P., Quirrenbach, A., Schalinski, C. J., Witzel, A., & Johnston, K. J. 1992a, *A&A*, 266, 93
 Hummel, C. A., et al. 1992b, *A&A*, 257, 489
 Koide, S., Nishikawa, K.-I., & Mutel, R. L. 1996a, *ApJ*, 463, L71 (KNM)

- Koide, S., Nishikawa, K.-I., & Mutel, R. L. 1996b, *J. Comput. Phys.*, submitted
- Koide, S., Sakai, J., Nishikawa, K.-I., & Mutel, R. L. 1996c, *ApJ*, 464, 724
- Komissarov, S. S., & Falle, S. A. E. G. 1996a, in *ASP Conf. Ser. 100, Energy Transport in Radio Galaxies and Quasars*, ed. P. E. Hardee, A. H. Bridle, & J. A. Zensus (San Francisco: ASP), 165
- . 1996b, in *ASP Conf. Ser. 100, Energy Transport in Radio Galaxies and Quasars*, ed. P. E. Hardee, A. H. Bridle, & J. A. Zensus (San Francisco: ASP), 173
- Krichbaum, T. P., Quirrenbach, A., & Witzel, A. 1992, in *Variability of Blazars*, ed. E. Valtaoja & M. Valtonen (Cambridge: Cambridge Univ. Press), 331
- Laing, R. A. 1996, in *ASP Conf. Ser. 100, Energy Transport in Radio Galaxies and Quasars*, ed. P. E. Hardee, A. H. Bridle, & J. A. Zensus (San Francisco: ASP), 241
- Martí, J. M^a, Font, J. A., Ibáñez, J. M^a, & Müller, E. 1996, in *ASP Conf. Ser. 100, Energy Transport in Radio Galaxies and Quasars*, ed. P. E. Hardee, A. H. Bridle, & J. A. Zensus (San Francisco: ASP), 149
- Martí, J. M^a, Müller, E., Font, J. A., & Ibáñez, J. M^a. 1995, *ApJ*, 448, L108
- Martí, J. M^a, Müller, E., & Ibáñez, J. M^a. 1994, *A&A*, 281, L9
- Mutel, R. L., Phillips, R. B., Su, B., & Bucciferro, R. R. 1990, *ApJ*, 352, 81
- Norman, M. L. 1993, in *Astrophysical Jets*, ed. D. Burgarella, M. Livio, & C. O'Dea (Cambridge: Cambridge Univ. Press), 211
- . 1996, in *ASP Conf. Ser. 100, Energy Transport in Radio Galaxies and Quasars*, ed. P. E. Hardee, A. H. Bridle, & J. A. Zensus (San Francisco: ASP), 319
- Qian, S. J., Quirrenbach, A., Witzel, A., Krichbaum, T. P., Hummel, C. A., & Zensus, J. A. 1991, *A&A*, 241, 15
- Qian, S. J., Witzel, A., Kraus, A., Krichbaum, T. P., & Britzen, S. 1996, in *ASP Conf. Ser. 100, Energy Transport in Radio Galaxies and Quasars*, ed. P. E. Hardee, A. H. Bridle, & J. A. Zensus (San Francisco: ASP), 55
- Stone, J. M., & Norman, M. L. 1992, *ApJ*, 389, 297
- van Putten, M. H. P. M. 1993, *ApJ*, 408, L21
- . 1996, *ApJ*, 467, L57
- Wardle, J. F. C., & Aaron, S. E. 1996, in *ASP Conf. Ser. 100, Energy Transport in Radio Galaxies and Quasars*, ed. P. E. Hardee, A. H. Bridle, & J. A. Zensus (San Francisco: ASP), 123
- Yokosawa, M., Ikeuchi, S., & Sakashita, S. 1982, *PASJ*, 34, 461

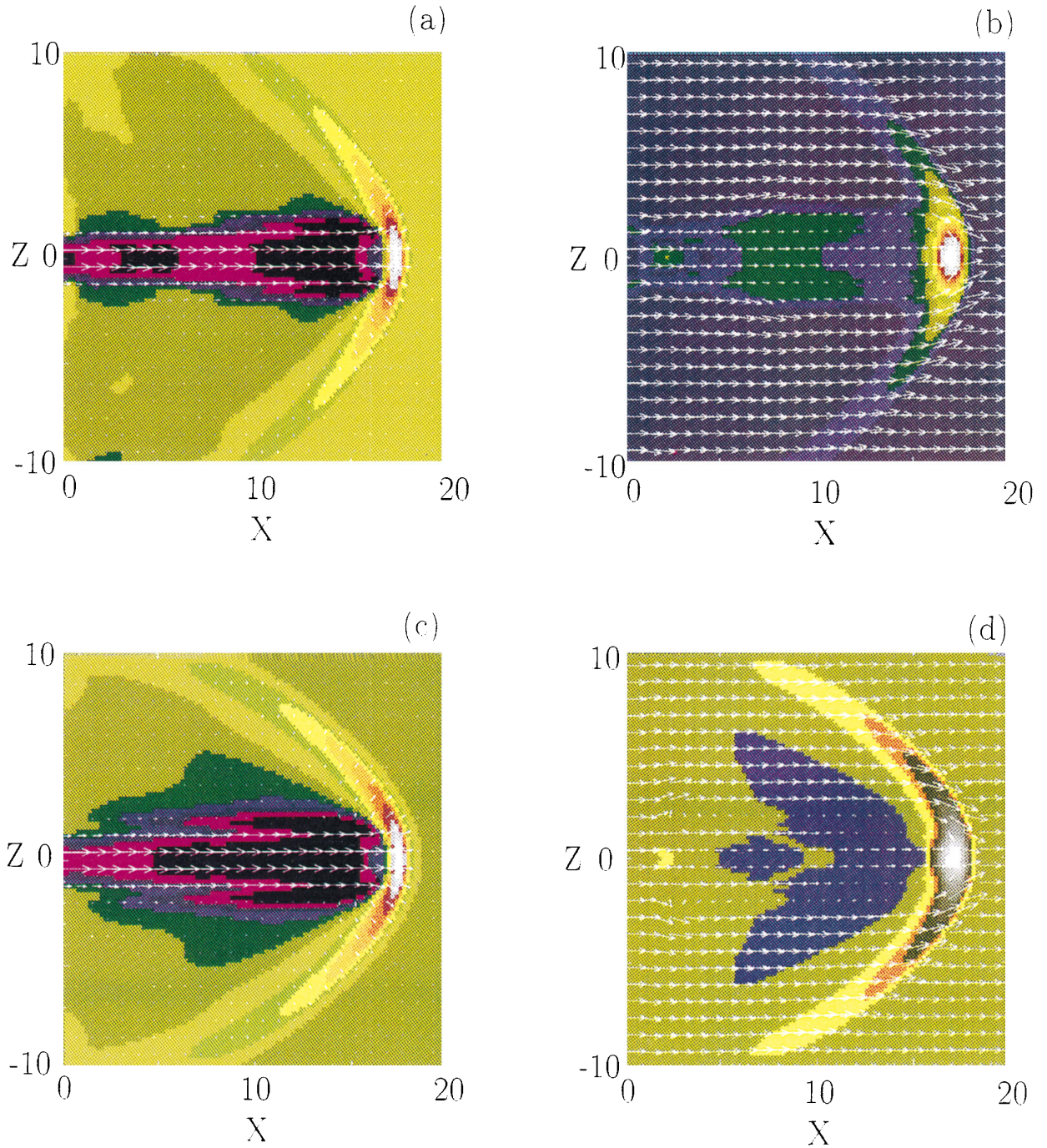


FIG. 1.—(a, b) Run A and (c, d) run B with strong and weak magnetic field, respectively: XZ cross sections through $Y = 0$ at $t = 8.5\tau_s$. (a, c) Contours of rest mass density and velocity vectors; (b, d) contours of thermal pressure and magnetic field vectors. The maximum values represented by white color are (a) $\rho_{\max} = 1.94$; (b) $P_{\max} = 3.29$; (c) $\rho_{\max} = 2.17$; and (d) $P_{\max} = 3.64$.

NISHIKAWA et al. (see 483, L46)

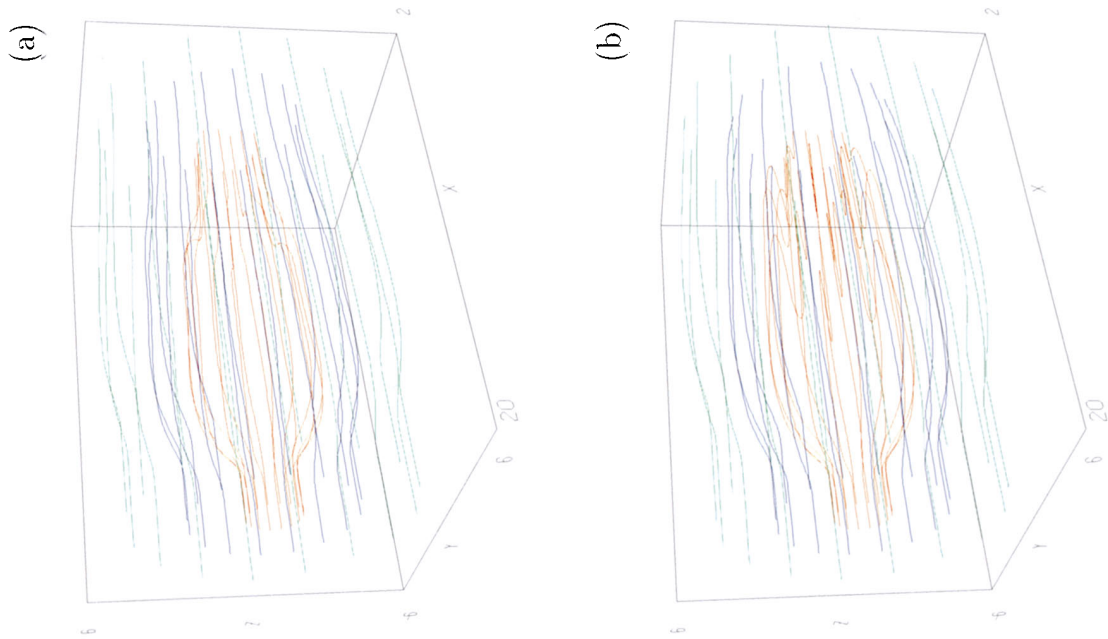


FIG. 2

FIG. 2.—(a) Run A and (b) run B: field lines in three-dimensional space at $t = 8.5\tau_s$ from a viewpoint in front and to the side of the jet. The red, blue, and green lines are traced starting at the front side ($X = 19.8$) from a radius of $(Y^2 + Z^2)^{1/2} = 1, 3$, and 5, respectively.

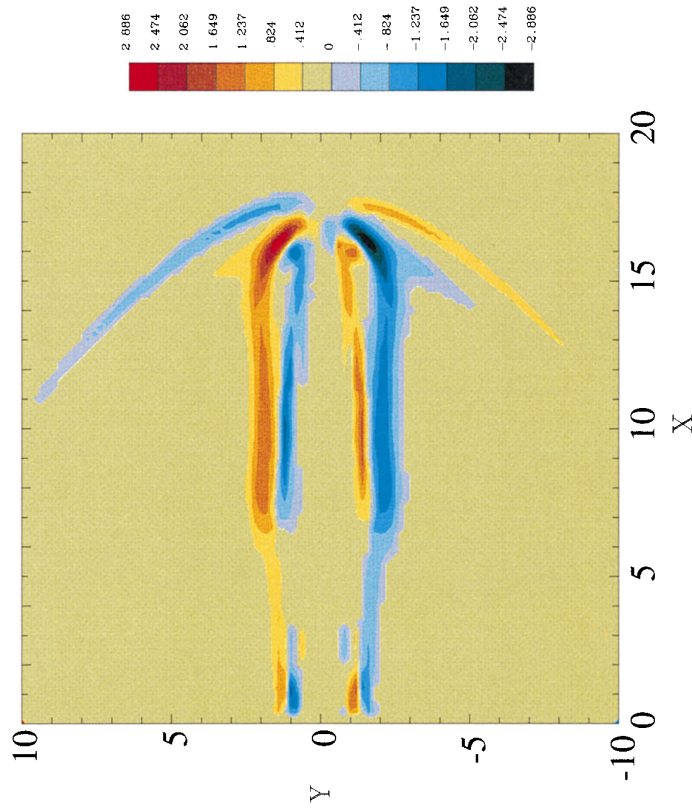


FIG. 3

FIG. 3.—Horizontal (XY) cross section through $Z = 0$ at $t = 8.5\tau_s$ for the strongly magnetized run showing the distribution of three different electric currents (J_z). The currents shown in red/blue color recede/approach the observer. Two currents circle near the surface of the cylindrical beam, and a third current circles around the bow shock.

NISHIKAWA et al. (see 483, L47)